International Journal of Impact Engineering, Volume 80, June 2015, pp. 203-211
DOI:10.1016/j.ijimpeng.2015.03.002

On the ballistic response of an aerospace-grade composite panel to non-spheroidised fragment simulants

G. J. Appleby-Thomas[1], D. C. Wood[1], A. Hameed[1] and J. A. Leighs[1]

[1]Centre for Defence Engineering, Cranfield University, Defence Academy of the United Kingdon, Shrivenham, Swindon, SN6 8LA

Abstract

The low mass and high specific strength of composite systems has led to their widespread adoption in aerospace applications. Consequently their performance under impact from off-normal events, or even deliberate insult, for example from a munition such as an anti-aircraft missile, is of paramount importance. Experimental and computational work to-date has typically focused on the response of composite systems to impact from projectiles with simple spherical or cylindrical geometries. However, such geometries are not representative of the full range of likely threats. In addition, even within this simple set of constraints the effects of projectile geometry on composite response under impact have been highlighted. Here an attempt has been made to investigate the effect of more complex geometric structures – comprising two-dimensional flat and peaked-nosed structures – on composite systems. A series of ballistic tests were carried out accelerating various geometric 'fragment simulants' into an aerospace-grade composite material. Damage was monitored in real time using high-speed cameras. Resultant calculations of projectile energy loss in the target, combined with analysis of recovered material via ultrasonic c-scan, have shown a clear relationship between projectile geometry and CFRP failure mode.

* Corresponding author. Tel.: +44 (0) 1793 785731. E-mail address: g.applebythomas@cranfield.ac.uk

Keywords: CFRP; ballistic impact; fragment geometry

1. Introduction

Both cost savings and performance improvements can result from weight reduction, providing a constant drive to minimise the mass of aerospace structures. Consequently, composite materials which combine low mass with high specific strengths are becoming ever more prevalent in the aerospace industry [1, 2]. In-service, aerospace systems are vulnerable to impact events of either natural or artificial origin (e.g. hail or MANPAD anti-aircraft systems, respectively). Such impact events may occur in the ballistic or hypervelocity (> 2 km/s) regime [3, 4]. Here, lower velocity 'ballistic impact' events such as collision with hail stones or shrapnel from anti-aircraft munitions, are considered.

These threats necessitate an understanding of the impact response of aerospace materials. This requirement has been recognised in recent years by a number of reviews. Cantwell and Morton [5] provided an overview of the impact response of numerous continuous fibre-reinforced composites. Consideration was given to six factors affecting composite response, namely: fibre properties; matrix properties; interphase properties; the nature of fibre stacking and the geometry of the composite. In particular, the importance of the interphase (the bonding region between the matrix and fibres) was highlighted. For example, if only a single projectile needs to be stopped then a weaker bond would be desirable, as this would allow for fibre/matrix delamination and subsequent energy dissipation. However, if post-impact properties were to be maximised, then a stronger bond would be required; consequently a trade-off in properties would likely be required for real-world applications. In a similar way, high strain-to-failure (smaller diameter) fibres were shown to provide increased ballistic resistance. However, the fact that reducing fibre diameter also reduced compressive strength was highlighted.

In addition, Cantwell and Morton [5] found the effects of geometry to be important, as energy absorbing capability did not always scale with target volume; with factors such as the curvature of a target shown to influence damage evolution. Further, rate-dependant behaviour was noted, with areal geometry becoming less important at higher rates-of-strain. For example, specimens of 50 mm and 150 mm length were impacted and analysed via C-scan, showing negligible differences in the levels of damage present in each [6].

More recently, Hazell and Appleby-Thomas [7] conducted a review of the literature focussing on the impact response of structural composite materials. This review detailed the key factors influencing both carbon and glass fibre-based composite systems. The authors highlighted that the vast majority of research to-date has suggested that, for two-dimensional composites, fibre lay-up and sequence are only influential at relatively low impact velocities (shown previously, for example, by Fuji et al. [8] and Tanabe et al. [9]). An example of this behaviour was published in a study by David-West et al. [10], in which two different composite lay-ups were subjected to impacts by hemispherically-nosed projectiles via a drop-tower. The resultant data showed that, in this relatively low velocity regime, the 0/45/90 layup was less resilient to this form of assault, when compared to tests on a 0/90 layup employing the same impact conditions. Conversely, at higher impact velocities, penetration has been found to be relatively independent of the nature of the composite lay-up. Advantageously, Hazell and Appleby-Thomas [7] also presented information from the literature, which concerned the ballistic response of composites at low temperatures. In particular, they highlighted the fact that beyond the ballistic limit, energy absorbing capabilities of CFRPs are comparable to those at room temperature. This is a significant factor for aerospace systems, where low temperatures would be expected during normal in-service life.

The majority of the aforementioned experimental studies into the ballistic response of composites has centred on the effects of relatively simple projectile types [7, 11-13]. For example, Cantwell and Morton [11] considered the effects of 6-mm diameter, 680 g hemispherically-nosed (driven at low velocity by a drop tower) and spherical, 6-mm diameter, 1 g projectiles (saboted projectiles driven to a high velocity by a light gas-gun) on different CFRP laminate geometries. They found that the loading strain-rate had a significant effect on composite response, with geometric factors key at lower velocities where elastic effects were important. Whereas at higher velocities, localised damage independent of factors such as target extent, were more prominent. This result was consistent with the general conclusions reached by Hazell and Appleby-Thomas [7], with regards to the influences of composite lay-up.

As already discussed, many researchers have employed spherical or hemisperically-fronted projectile arrangements in a similar manner to Cantwell and Morton [11]. These include Hazell et al. [12] who studied the effects of thickness and obliquity on woven CFRP performance when impacted with 11.97-mm diameter, 7.2 g annealed steel spheres. In this study, targets were impacted at velocities in the range 170 to 374 m/s and high-speed video was employed to monitor the impact events. A transition in failure mode from petalling at lower impact velocities to plug formation (shear) at higher velocities was observed, consistent with the strain-rate effects observed previously by Cantwell and Morton [11]. This correlated to a ballistic advantage in terms of kinetic energy absorbed per unit of composite thickness for thicker CFRP systems at lower impact velocities. This behaviour was attributed to the fact that the incident projectile required more energy to push the petals formed in thicker composites out of the way during penetration, as opposed to situations where thinner composites were impacted. However, at elevated impact velocities where petalling was no longer the dominant failure mode this advantage rapidly diminished. Further, while Hazell et

al. [12] found evidence of enhanced performance for inclined CFRP targets, when penetration was normalised for the resolved thickness of the inclined targets the increased ballistic resistance was found to be entirely attributable to this geometric effect.

López-Puente et al. [14] also studied the effects of obliquity on the resilience of carbon/epoxy woven laminates. Targets angled at both 0° and 45° were impacted by 1.73 g steel spheres at velocities between 70 and 531 m/s via the employment of a gas gun. In line with other studies published in the literature, a high-speed camera was used to measure residual velocities. Below the ballistic limit, López-Puente et al. observed that the damage caused to targets at both angles increased with impact velocity, however above this limit, the opposite behaviour was noted. Results also showed that the ballistic limit increases with the obliquity of the target. Below the ballistic limit, greater levels of damage were seen in the 0° targets; however, at higher velocities, damage observed in 45° targets was shown to be greater than in the 0° arrangements. The authors attributed this behaviour to a change in the governing damage mechanism at the ballistic limit; below, delamination was the key mechanism whereas above, it was projectile piercing.

In a similar study to Hazell et al. [12], Caprino et al. [13] investigated the ballistic response of various thicknesses of stitched CFRP materials, designed to be more resistant to delamination than un-stitched systems. Targets were impacted with 12.7 and 20-mm diameter projectiles at nominal impact velocities of 129 and 65 m/s, respectively. In concord with the results from Hazell et al. [12], employing low impact velocities (comparable to those tested here), the perforation energy was found to increase non-linearly with panel thickness. This suggested a ballistic advantage for thicker panels in this velocity regime, presumably resulting from the failure mode in operation. Ultrasonic c-scan analysis of the impacted composites showed a number of interesting features: (1) stitching was found to inhibit subsurface delamination in places, with the failure contours following the stitching itself, and;

(2) delamination was found to have a circular form with thicker plates and an elliptical nature (oriented along the fibre-direction) with thinner panels, suggestive of a thickness-dependant change in failure mode. In addition, experimental data was found to be in good agreement with two models from the literature [15, 16].

Robinson and Davies [17] conducted a series of tests in which woven fibre reinforced composite laminates were impact with projectiles of a variety of masses. One of the main aims of this study was to observe the effects, if any, varying mass alone had on the stress distributions close to the impact point and the damage mechanisms present. The results of these tests showed that at the low velocities employed here both the damage seen and the peak force was purely a function of the impact energy, i.e. the combined effect of both mass and velocity, rather than either being solely responsible.

Other researchers have looked at the effects of cylindrical projectiles on composite systems [18, 19, 22]; these tests have often been carried out to aid in the validation of numerical models, as such projectiles ensure uniform contact area on the target composite. There have been numerous attempts to produce numerical models which enable simulation of the impact response of composite systems [18, 20-23]. However, these have been complicated by the structural complexity inherent in such arrangements. Wen [18] derived a series of equations which allowed prediction of changes in penetration and ballistic limit of fibre reinforced polymers under impact from both flat, hemispherical, ogive and conically-shaped projectiles. However, only limited comparison to disparate literature data was made, with the assumption of localised damage on impact. Consequently, while a useful predictive tool, only limited insight into the physical nature of CFRP failure could be drawn. In a recent paper building on previous studies [20, 21], Shaktivesh et al. [22] developed a numerical model based around an energy balance approach, in which a projectiles kinetic energy was equated to the various potential damage and energy absorbing mechanisms. The mechanisms studied were

primarily shear plugging, compression of the composite yarns and tensile failure of elements of the composite. Penetration was considered to occur in three phases: (1) initial compression on impact – with compressive longitudinal and shear waves propagating through the composite, leading to local failure where material strength is overcome; (2) wave arrival at the rear face of the composite – potentially leading to conical deformation and consequent tensile loading of un-failed fibres, and; (3) frictional interaction between the projectile and failed composite material. Simulations from the numerical model were compared to a series of ballistic tests in which a relatively simple projectile configuration was assumed. The validation experiments involved six 4.25-mm thick, 125 mm × 125 mm, 2D plain weave e-glass/epoxy composites being impacted normally by cylindrical flat-ended 5.0 g, 6.35-mm diameter hardened steel projectiles. A V_{50} ballistic limit of 148 m/s, with a velocity range of 145 to 152 m/s was established. This was in excellent agreement with the predicted value calculated using the aforementioned energy balance approach of 155 m/s. Interestingly, further application of this numerical model implied that shear plugging was typically the dominant energy absorbing mechanism under such planar cylindrical-projectile loading conditions. However, despite the excellent agreement between experiment and simulation, the authors did not extend their model to situations involving more complex projectile shapes.

Varas et al. [23] have detailed a similar study, although in this case using the commercially available computational code ABAQUS/Explicit. This approach allowed simulation of sub-surface delamination via the use of cohesive elements. In line with the approach taken by Shaktivesh et al. [22], Varas et al. undertook a series of gas-gun experiments to provide data to help validate their simulations. These tests involved impacts in the range 100 to 400 m/s of 5.5-mm diameter, 1.1 g tempered steel cylindrical projectiles onto 2.0-mm thick, 80 mm^2 carbon/epoxy laminated targets consisting of 10 plies in a uni-directional lay-up. In this case, the assumption was made that the hardness of the chosen tempered steel projectiles

overmatched that of the CFRP – e.g., they were assumed to be sufficiently hard that no plastic deformation of the projectile occurred during the impact event. As well as recording impact and residual post-penetration projectile velocities via high speed camera, post-mortem analysis of subsurface damage via ultrasonic c-scanning (similar to the approach adopted by Caprino et al. [13]) provided information on material delamination following impact. The computational models involved a number of key elements, with the projectile material model taken as linear-elastic, in line with the non-deforming nature of the projectile and the composite material modelled as an orthotropic elastic material to the point of failure. Composite failure was simulated based on both intra- and inter-laminar behaviour. Intra-laminar behaviour, based on a user-defined subroutine, accounted for both the anisotropic nature of fibre failure in a woven composite and crushing of the surrounding matrix under impact. Inter-laminar failure – essentially the evolution of regions of sub-surface delamination – was modelled by introducing a plane of cohesive elements in the centre of the 10-ply system with associated failure criteria. The simulations were found to provide a strong match to residual projectile velocities in the experimental data, within the impact velocity range under consideration; both experiment and simulation suggested a ballistic limit of ~ 140 m/s. The match between the measured (via c-scan analysis) and computationally simulated sub-surface delamination was not quite as consistent as the prediction of projectile residual velocity. However, this was perhaps unsurprising given the simplifying assumptions inherent in the model (for example, the assumption of delamination in the central region only) and the authors highlighted similarities in the general trends in both the experimental and simulated data. The validated computational model was subsequently employed to interrogate the effects of projectile diameter on residual velocity. Projectile mass and velocity (and therefore kinetic energy) were kept constant while the projectile aspect ratio was changed. Smaller diameter projectiles were found to lead to a lower ballistic limit. This

observation is consistent with the accompanying increase in kinetic energy-density on impact, which was linked to the differing failure mechanisms, such as laminate crushing on impact. This result accentuates the importance of projectile properties in predicting the impact response of a composite system. For example, even with this simple cylindrical geometric structure, varying projectile aspect ratio had a substantial effect on subsequent composite ballistic response.

The idea of parametrically investigating projectile parameters, employed by Caprino et al. [13] (albeit for just two diameters of steel sphere), is of particular note as it has the potential to provide a predictive capability for a much wider variety of impactor types. As detailed above, the vast majority of experimental work to-date has focused on very simple projectile geometries, namely spheres or cylinders. These are, however, unlikely to be representative of the full range of threats that, for example, an aerospace structure might encounter (e.g. angular fragments from a MANPAD etc.). Consequently, in this study, the authors have focused on extending the data presented in the literature to facilitate understanding of the ballistic response of composite systems to more complex geometric projectiles. Similar to the broad approach taken by Caprino et al., this study has employed a wide range of impactor geometries in order to ascertain the effects of a more representative group of simulated fragments.

2. Experimental

A 22-mm bore, 1.5 m barrel, single-stage gas-gun was employed for all experiments. Projectiles consisting of 6-mm thick 304L stainless steel plates, with widths of 12 mm, were placed in acetal sabots and accelerated at velocities between 92 and 288 m/s into 90 mm × 90 mm (± 5 mm) square CFRP arrangements. In in line with the approach adopted previously

by Varas et al. [23], this projectile material was chosen to overmatch the target, ensuring minimal plastic deformation on impact. The chosen composite, supplied by Short Brothers plc. (Belfast), comprised 3.5-mm thick (1.51 g/cc – measured via Archimedes' principle using a Mettler Toledo X5105 balance) 8 ply laminates. The preform consisted of alternating layers of Triaxial and UD NCF aero-grade fibres, with a lay-up of the form (0/90, ±45, ±45, 0/90, 0/90, ±45, ±45, 0/90). The matrix, formed via the Resin Transfer Moulding (RTM) method, consisted of RTM6 [24] cured for 1 ½ hours at 180 ºC and 80 psi, with a 2 hour post-cure carried out at 180 ºC. A Phantom V.7 high-speed video camera was employed to monitor impacts, operating at c.a. 25,000 frames-per-second. Calibration against a scale allowed direct measurement of projectile velocities both on impact and post-penetration. This then allowed subsequent calculation of the kinetic energy transferred to the target (ΔE_{KE}) via the relation,

$$\Delta E_{KE} = \frac{1}{2} m_P \left(v_i^2 - v_f^2 \right) \quad (1)$$

Where, for the projectile in question, m_P is the mass and v_i and v_f are the impact and post-impact velocities respectively.

Target CFRP panels were fixed securely within a mounting frame, with restraint applied along the top and bottom edges only. To achieve this, each target was mounted such that the rear surface of the outer ca. 5 mm of the upper and lower target edges was placed against a backing comprising box-section steel tube. Metal flanges secured by retaining bolts were than used to hold these surfaces in place, leading to a free target area of 80 mm × 90 mm.

Assuming central impact, this provided a minimum target width equivalent to 6 2/3 times the projectile diameter (12 mm). This was judged sufficient to ensure semi-infinite behaviour, while making optimum use of available composite materials. While c-scan data indicated that delamination reached to the outer edge of the target where a 180° (flat) projectile was employed at 185 m/s, it seems likely that this also occurred in the other 180° case despite the lower impact velocity of 166 m/s. Nevertheless, even at 185 m/s, the resultant damage at the outer target edge was non-catastrophic and sub-surface delamination, while apparent at three target edges, was beginning to reduce in lateral extent. Consequently, apart from the two 180° shots it was felt that this decision to employ 90 mm × 90 mm targets has minimal effect on resultant target behaviour. This setup is shown schematically in Fig. 1. In all cases, careful observation of the high speed video footage recorded during experiments showed no evidence of target movement until after the penetration event had occurred.

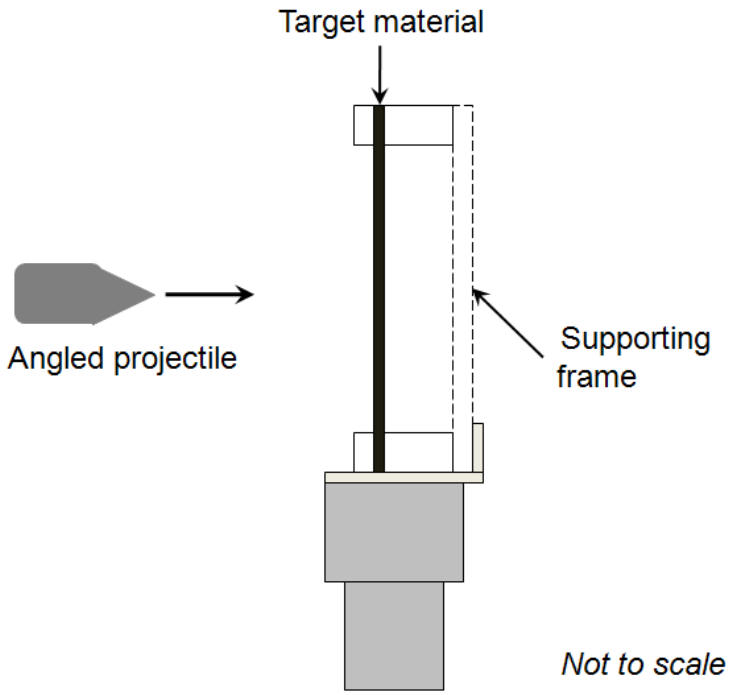

Fig. 1. Experimental setup.

The main projectiles employed consisted of two 304 steel structures with either planar or angled end sections. In addition, for one test a 304 stainless steel sphere of 12-mm diameter and 7.165 ± 0.001 g mass was used (the same projectile type employed in previous in-house tests on composites [12, 25, 26]). Key planar projectile parameters along with an illustration in-profile of each of the manufactured planar projectile types employed are set out in Table 1. Projectile dimensions were selected such that the mass remained constant between projectiles sets. All projectiles were mounted in 22-mm diameter acetal sabots which were stripped before the projectile impacted the mounted target as-shown in Fig. 1.

Table 1. Details of projectile employed (nominally 12.0 mm diam. / 6.0 mm depth): 14.9 ± 0.1 g.

Tip angle (degrees)	Overall length (mm)	Length of tip (mm)	
180.0	27.5	0.0	
100.4	30.0	5.0	
61.9	32.5	10.0	
33.4	37.5	20.0	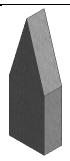

3. Results and discussion

As detailed in Table 1, a total of 4 different projectile configurations were considered. Saboted projectiles were impacted at velocities between 98 and 288 m/s in a total of 13 impact experiments designed to provide an insight into the influence of different facets of projectile architecture on penetration. In all cases, targets comprised 90 mm × 90 mm 3.5-mm thick 8 ply laminates. Key experimental parameters and results are detailed in Table 2.

Table 2. Experimental results.

Projectile type / mass (g)	Impact velocity (m/s) / KE (J)	Residual velocity (m/s) / KE (J)	Percentage change in KE (%)	Delaminated area from C-scan data (mm^2)
Sphere	267 / 284	233 / 217	67.1	----
2D 180º	166 / 204	132 / 129	36.9	----
	185 / 253	152 / 174	32.0	66.0
2D 100º	132 / 130	98 / 71	45.4	----
	173 / 222	153 / 173	28.9	----
	183 / 247	156 / 181	26.6	25.2
	288 / 617	269 / 538	12.9	----
2D 62º	128 / 122	88 / 58	52.8	34.3
	179 / 237	151 / 169	28.8	31.2
	182 / 244	154 / 174	28.9	----
	237 / 416	220 / 356	45.6	----
2D 33º	186 / 261	170 / 217	16.7	----
	182 / 247	163 / 198	19.9	17.5

High-speed video footage for the four 2D projectile impacts which occurred at 181.9 ± 2.4 m/s (c.a. 250 J) into the target laminates for which c-scan data was subsequently gathered (Fig. 5 / as in detailed in Table 2) is presented in Fig. 2.

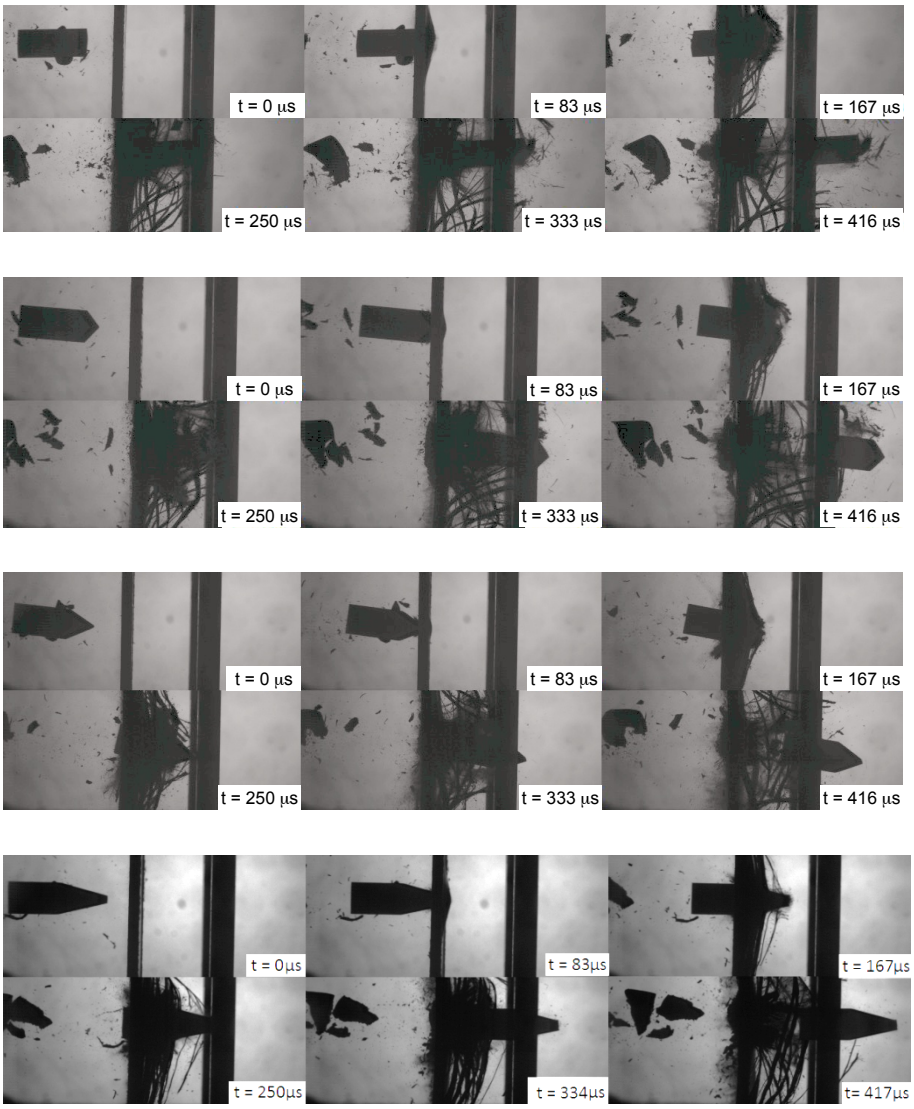

Fig. 2. High-speed video footage illustrating impact of 2D projectiles of varying geometry into CFRP targets.

In all cases in Fig. 2, at 0 μs the projectile is visible just before impact, with the composite panel situated directly to its right and beyond this, towards the right-hand edge of the image, an upright element of the retaining frame. It is notable that several of the projectiles show a

measurable degree of yaw. This has been attributed to the interaction of the acetal sabot employed to encase the projectile on launch with the sabot stripping arrangement. This misalignment of the projectile has been measured (using the freeware software package ImageJ) across the captured HSV footage as being a maximum of 6.40° relative to the target normal, with a mean value of 3.90° ± 2.60. However, while observable in the HSV footage, this effect did not appear to greatly influence the resultant behaviour (e.g. as shown later in Fig. 5, sub-surface damaged scaled with impact velocity independent of any misalignment issues). This was assumed to be because with 'pointed' projectiles such small misalignment angles were insufficient to prevent the key geometric feature – namely the projectile tip – impacting before the main body of the projectile. This factor is clearly illustrated in Fig. 2(b) which shows the worst-case misalignment of 6.40° – but with the sculpted projectile tip still impacting first. Consequently, this effect has been neglected in subsequent discussions. Sabot fragments which have worked their way through the stripping arrangement are visible in all images – particularly at later times. Sabots were typically of a comparable mass to the projectiles themselves, with a nominal mass of 15 g. However, as the sabots consisted of low density (and brittle) acetal, they fragmented on impact into small sections – with the largest section comprising the solid backing element used to support the projectile. This section weighed less than 5 g and because it had been slowed by impact with (and fragmentation at) the sabot stripper always had a velocity very much less than that of the main projectiles – with velocities as low as 30 m/s recorded. Consequently, it was found that these fragments had no discernable effect on the composite structure and did not contribute meaningfully to the penetration mechanisms under consideration here.

In the captured video footage shown in Fig. 2, the first significant differences in penetration behaviour occur following the 167 μs frame. With the blunt nosed projectile employed in Fig. 2a, substantial deformation/fragmentation of the target – likely arising due to crushing

and (potentially) plugging – is apparent ahead of the penetrating projectile at 167 μs, with some broken tows visible by 250 μs. However, as the projectile nose becomes sharper, there is evidence of a change in penetration mechanism, with penetration involving earlier fracture of the CFRP tows. For example, with the 62º projectile in Fig. 2c, broken fibres/tows are clearly visible at 167 μs, with less overall damage apparent than in the 180º projectile case in Fig. 2a. Moving to the most oblique-nosed projectile – 33º – in Fig. 2d, even less damage is initially apparent at 167 μs, suggesting more efficient penetration. Interestingly, this apparent behaviour appears to correspond with the transition to piercing at elevated impact velocities observed by López-Puente et al. [14] for sphere impacts on carbon/epoxy laminates. This conclusion that penetration becomes more efficient with enhanced projectile obliquity is backed up by the fact that the 33º projectile appears to have travelled significantly further beyond the target CFRP plate by 417 μs than is the case for the projectiles in Figs. 2a – 2c. More generally, such behaviour, with failure mode varying as a function of loading rate, has been observed elsewhere [11, 12]. For example, Cantwell and Morton [11] observed that pedalling transitioned to plug formation at elevated impact velocities – with fibres rapidly shearing post-impact.

Data showing the percentage change in KE following penetration for the 2D (planar) impactor experiments detailed in Table 2 is presented in Fig. 3a; with the absolute change in kinetic energy presented in Fig. 3b.

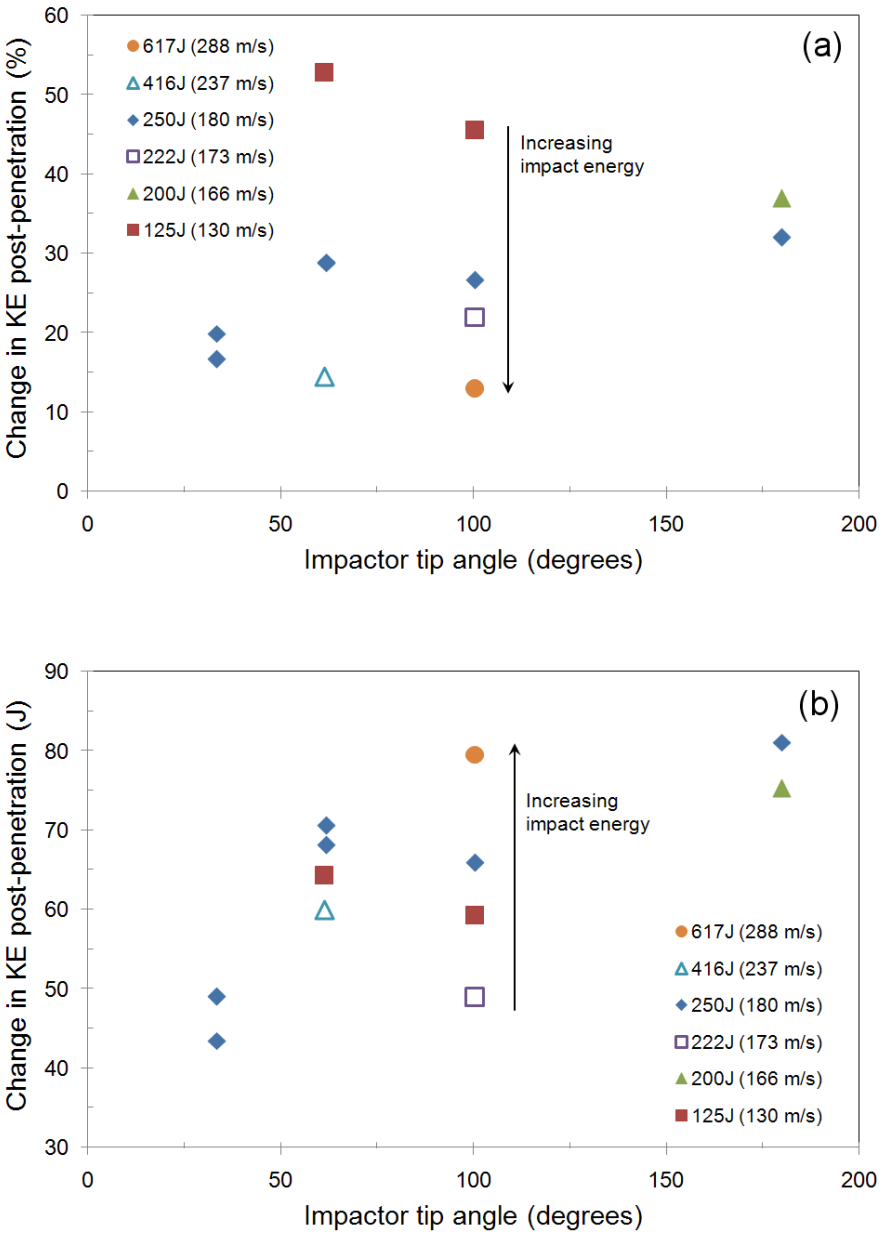

Fig. 3. Variation in kinetic energy loss with impactor geometry: (a) percentage change; (b) absolute change.

Two trends are immediately apparent from the results presented in Fig. 3. First of all, despite the inherent experimental scatter encountered in any ballistics-related test, from the 250 J (c.a. 180 m/s) data presented in both figures, it is clear that increasing the sharpness of the projectile tip leads to an essentially linear reduction in both relative (percentage) and absolute kinetic energy loss following impact. This suggests that, as might be expected, sharper,

narrower, projectiles penetrate more efficiently. In other words, such sharper-nosed projectiles are able to 'pierce' [14] the target, as opposed to relying on plugging/sear to cause failure. However, this transition in failure mode does not appear to be discrete. It is interesting to note that there appears to be some evidence of a change in energy dissipation mechanism between the 62º and 100º results – manifested as an apparent change in gradient in the underlying trend for the 250 J data for both figures.

In addition, in the percentage change in kinetic energy results presented in Fig. 3a, both the 62º and 100º data sets – where several impact velocities/energies were considered for a single geometry projectile – appear to indicate an additional underlying trend. There appears to be a general tendency for penetration with a given geometry of penetrator to become more efficient as impact energy increases. This is reflected by the arrow in Fig. 3a, which shows a general trend of a lower overall percentage change in KE being required to achieve penetration as initial kinetic energy is increased for the 100º case. In this context, it is worth noting that while the 225 and 250 J results (for a tip angle of 100º) appear to be out of sequence, as shown in Table 2, there is just 10 m/s between the measured velocity for both of these shots. This suggests that these co-incident results sit within the likely experimental error. However, this apparent relationship between impact energy and kinetic energy change takes the opposite form in Fig. 3b, where the absolute change in kinetic energy of the incident projectile following impact is considered. In this case, the general trend appears to be one of increasing absolute energy loss with increasing impact energy. This does not appear to be linked to the variation in impact energy as set out in Table 2, as impact energy varies by just 9 J across the entire sample set – with only a 6 J difference in impact energy between the extreme 180º and 33º cases. Instead, on further examination, this discrepancy appears to be linked to the fact that the overall absolute energy loss in all cases is actually relatively small – sitting in a range between 45 and 80 J. Consequently, particularly given the fact that the

behaviour at differing impact velocities/energies for fragment angles of both 62º and 100º is substantially less well defined than that illustrated in Fig. 3a, it is postulated that this difference in apparent behaviour is a function of the nature of energy dissipation. In other words, at higher velocities more energy will be dissipated in plastic deformation of the impactor as well as in light and heat on impact leading to a larger absolute energy loss as shown in Fig. 3b. Conversely, as shown in Fig. 3a, the higher the impact energy the lower the percentage of the projectiles initial kinetic energy lost via such mechanisms for a given tip geometry. Interestingly, this suggests that as long as failure modes are similar, penetration will only take a finite amount of energy. Nevertheless, as highlighted previously, the similarity in the underlying trend for the 250 J data in both Figs. 3a and 3b demonstrates a clearly discernable effect of projectile geometry on penetration.

It is interesting to note that other authors have consistently dealt in terms of percentage change in energy post-impact rather than considering the absolute energy change. For example, Hazell et al. [12] considered energy dissipation following ballistic impact of spheres against two different thicknesses of CFRP. To this end, the data for a 3-mm thickness of CFRP with a similar weave to that considered here impacted with 12-mm diameter 7.2 g stainless-steel spheres is presented alongside that from Table 2 – including the test-shot carried out here with a similar steel sphere – in Fig. 4. Usefully, areal densities of the two different lay-ups are comparable. Areal density may be calculated as density multiplied by thickness for a given material [27]. To this end, here, the areal density of the CFRP panels considered is equal to 5.30 g/cm^2 (0.35 cm × 1.51 g/cm^3), compared to 4.54 g/cm^2 (0.3 cm × 1.51 g/cm^3) for the panels considered by Hazell et al. [12]. Consequently despite the differing panel thicknesses, a direct comparison of CFRP performance is reasonable.

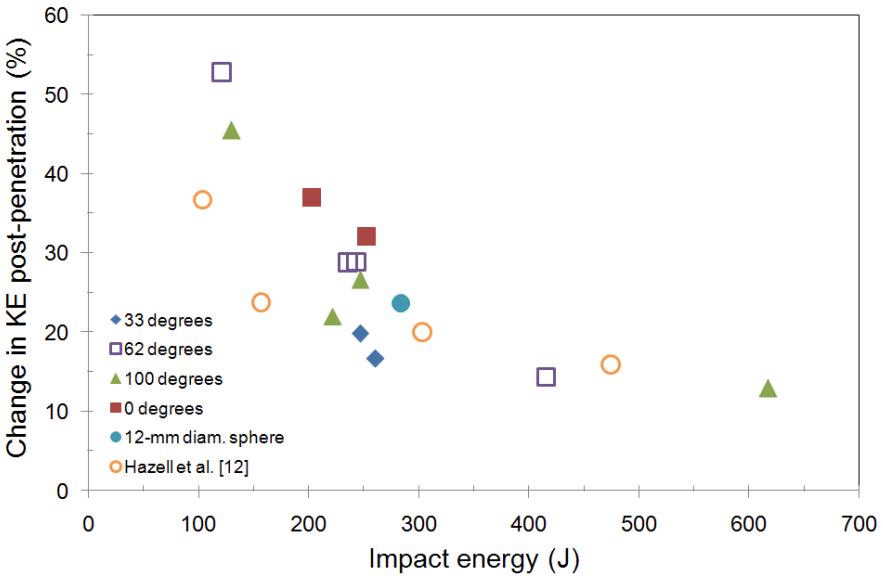

Fig. 4. Variation of change in kinetic energy post-impact (%) with initial projectile impact energy for the varying projectiles considered here, plus data from Ref. [12].

There are several observations which can immediately be drawn from Fig. 4. Firstly, for all the projectile configurations considered an (exponential) decrease in energy dissipation with impact energy is apparent; although as illustrated by Fig. 3, this does not automatically transfer into a change in absolute energy dissipated post-impact. Secondly, it is notable that there is good agreement between the single sphere-impact shot conducted on the CFRP panel considered here and the data for the thinner – but similar areal density – panel investigated by Hazel et al. This result backs the decision to employ this data here for the purpose of comparison. Thirdly, as in Fig. 3, a clear projectile architecture-dependant effect can be observed in Fig. 4. Around 250 J (corresponding to an impact velocity of c.a. 180 m/s for the planar projectiles primarily considered here), the separation in terms of KE change following impact for different projectile types previously highlighted in Fig. 3a is again apparent. Blunter nosed 180º projectiles appear to give up significantly more energy than the sharper 33º nosed projectiles; indicating that penetration is more efficient for the more oblique

projectiles. As highlighted previously, however, it is of note that the variation in KE change does not entirely scale with projectile nose angle – with the 62º and 100º data essentially co-incident. It is also interesting to note that the residual energy data for spherical projectiles (both from the single test highlighted in Table 2 and from Ref. [12]) in this region appears to sit somewhat above the 33º projectile data. This backs the general conclusion that projectile geometry does indeed affect penetration efficiency in such composite targets.

To investigate the extent of sub-surface damage, a selection of recovered samples were analysed using ultrasonic c-scanning equipment. Ultrasonic c-scans for the four targets shown in Fig. 2 (impact velocity c.a. 180 m/s – corresponding to an impact energy of c.a. 250 J) are presented in Fig. 5.

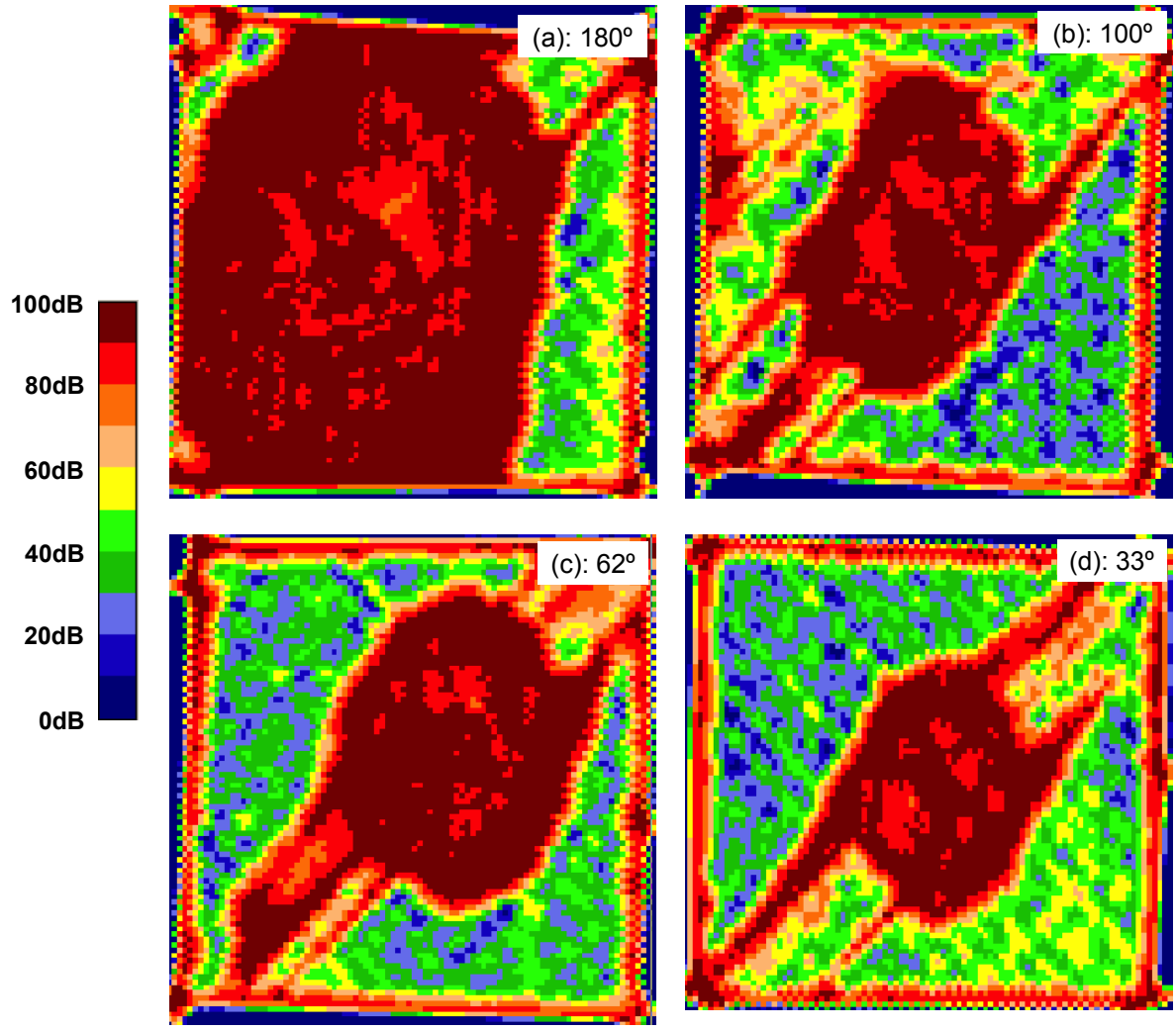

Fig. 5. Ultrasonic C-scans of CFRP targets impacted with 2D projectiles of varying obliquity: (a) 185 m/s; (b) 183 m/s; (c) 179 m/s, and; (d) 182 m/s.

The c-scans presented in Fig. 5 show a number of interesting features. Firstly, in all cases there is clear evidence of a central region of delamination with outlying linear regions corresponding to delaminated plies. However, interestingly, this outer delamination demonstrates a clear asymmetry with a clear underlying directionality. This behaviour manifests as delamination occurring in all cases along a 2D strip, consistent with the 2D geometry of the impacting projectiles (all scans have been rotated to show this region running from the bottom left to top right in Fig. 5 for clarity). However, it should be noted that the

panels considered here are relatively thin and, interestingly, Caprino et al. [13] have previously noted elliptical damage areas following the fibre direction even with spherical projectiles where thin target panels were employed. This sub-surface damage subsequently moved to more spheradised damage regions as panel thickness increased; with this behaviour tentatively attributed to a thickness-dependant variation in failure mode. Nevertheless, the consistent nature of damage modes in Fig. 5 strongly suggests that they are linked to the geometry of the projectiles in this case. The second feature which is apparent from Fig. 5 is that, in general, there is a decrease in damage extent as the penetrator tip obliquity decreases. Although these scans do appear to suggest a slight increase in the extent of damage moving from a projectile nose angle of 100° to 62°, before damage extent reduces further for the target impacted by a 33° tip projectile. This behaviour, which is consistent with the previously highlighted apparent change in failure mode in Fig. 3, is shown in more detail in Fig. 6, where damage areas measured from Fig. 5 are compared.

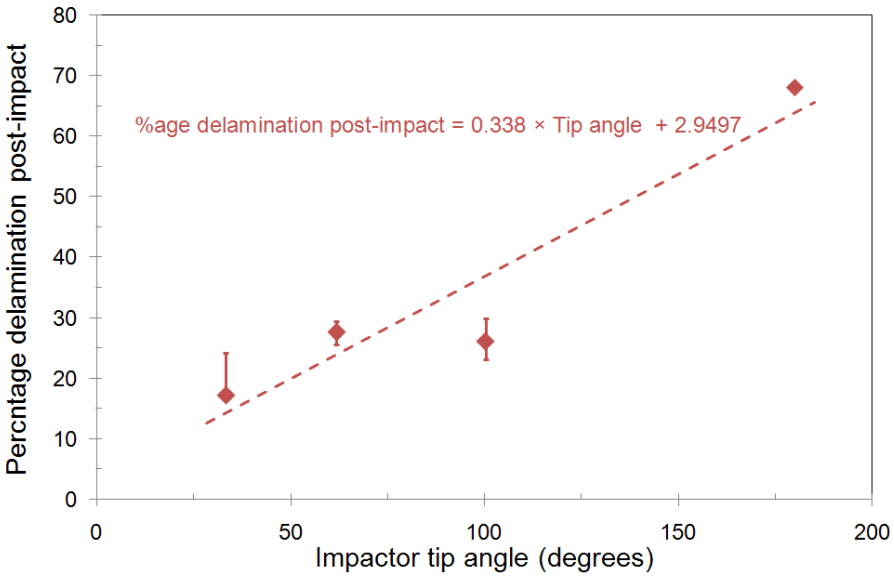

Fig. 6. Measured delamination (by c-scan) resulting from impact at ca. 180 m/s by 2D imapctors of varying tip angle.

It should be noted that data from just four c-scans has been considered here, making quantitative assessment as to the presence of features such as the aforementioned change in failure mode in the interval between 100° and 62°challenging. Nevertheless, Fig. 6 does seem to show clear evidence of a decrease in the degree of sub-surface damage (as detected by ultrasonic c-scan) as the obliquity of the projectile tip increases. In essence, in line with the plots presented previously in Fig. 3, sharper projectiles appear to penetrate more effectively – with less resultant damage (and therefore as outlined in Fig. 3, less percentage and absolute energy loss) – compared to less sharply-tipped projectiles. This is conceptually a simple effect, but it highlights a key issue with regards to the importance of understanding both the target and projectile during CFRP attack/defeat. Authors such as Caprino et al. [13] and Varas et al. [23] have investigated the effects of projectile diameter (in the latter case via simulations), while Robinson and Davies [17] investigated the influence of projectile mass and others such as Wu et al. [19] have looked at the influence of moving to a cylindrical projectile. However, to the authors' knowledge, no previous systematic experimental study of the effects of projectile geometry on CFRP penetration has been undertaken. Wen [18] derived a series of analytical equations allowing prediction of depth of penetration into fibre reinforced polymers – however, comparison of the resultant models was only made to limited information from the literature. Nevertheless, the work presented here strongly suggests a link between projectile geometry and both (1) ease of penetration, and; (2) the nature/shape and extent of resultant sub-surface damage.

4. Conclusions

In this study the ballistic response of an aero-grade CFRP structure to impact with a selection of 2D planar projectiles with varying nose architecture has been studied. High speed video footage allowed both visualisation of the impact event and for projectile energy loss (and therefore energy transfer to the target) to be measured/calculated. Finally ultrasonic c-scans of selected targets have provided an insight into sub-surface material failure.

This study essentially comprised a systematic experimental investigation of the effects of projectile geometry on CFRP ballistic response. While other studies have looked at the effects of projectile mass and have considered both spherical and cylindrical projectiles, there is a paucity of experimental insight in the literature into composite response to insult with more complex geometric structures. While ultrasonic c-scanning was only conducted on a limited number of samples making qualitative analysis difficult, there was clear evidence of a geometric-linked response, with both the shape and extent of visualised sub-surface damage scaling with the form of the impacting projectile. As might be expected, more oblique (sharply nosed) projectiles were found to be more efficient at penetrating targets, leading to lower levels of sub-surface delamination post-impact (as measured by c-scan). Changes in both observed material response (using high speed video) and in the damage extent measured via c-scan provided limited evidence that there may have been a change in composite failure mode with projectile nose shape; however as outlined previously, c-scan data was only available for four shots, complicating analysis. Nevertheless, from the high speed video footage, it appeared that as the projectile nose became sharper, penetration seemed to move from crushing and tensile failure of the CFRP reinforcing fibres to cleaner shear/piercing. Further, comparison to literature data for the effects of spherical impactors on a comparable

CFRP structure indicated a substantial difference between composite response to spherical and 2D angular projectiles at similar impact energies.

Combined with evidence from c-scan data that sub-surface delamination had a general form consistent with the geometry of the impactor, these results were taken to suggest that projectile geometry does have a significant effect on composite failure. This is a critical issue as attack on CFRP structures (for example from a MANPAD or similar threat) is unlikely to come from a projectile of uniform geometric structure. Consequently, the study conducted here clearly demonstates the importance of not only understanding the effects of composite structure on ballistic response, but also the nature of the likely threat.

5. Acknowledgements

The primary author wishes to acknowledge the support of his wife, Caroline Appleby-Thomas, while writing this paper. In addition, it is noted that the majority of the experimental work reported here was undertaken in the course of an Explosives Ordnance Engineering MSc to by Mr Joshua Jenkins at Cranfield University's Shrivenham Campus in 2012/2013.

6. References

[1] Appleby-Thomas GJ, Hazell PJ, Dahini G. On the response of two commercially important CFRP structures to multiple ice impacts. Comp. Struct. 2011;93:2619-2627.

[2] Ryan S, Schäfer F, Guyot M, Hiermaier S, Lambert M. Characterizing the transient response of CFRP/Al HC spacecraft structures induced by space debris impact at hypervelocity. Int. J. Impact Engng. 2008;35:1756-1763.

[3] Fair H. Hypervelocity then and now. Int. J. Impact Eng. 1987;5:1-11.

[4] Schonberg WP. Protecting Earth-orbiting spacecraft against micro-meteoroid/orbital debris impact damage using composite structural systems and materials: An overview. Adv. Space Res. 2010;45(6):709-720.

[5] Cantwell WJ, Morton J. The impact resistance of composite materials – a review. Composites 1991;22(5):347-362.

[6] Su KB. Delamination resistance of stitched thermoplastic matrix composite laminates. In: Newaz GM, editor. Advances in Thermoplastic Matrix Composite Materials, ASTM STP 1044. American Society for Testing and Materials, 1989. p. 279-300.

[7] Hazell PJ, Appleby-Thomas GJ. The impact of structural composite materials. Part I: ballistic impact. J. Strain Analysis for Eng. Design 2012;47(7):396-405.

[8] Fuji K, Aoki M, Kiuchi N, Yasuda E, Tanabe Y. Impact perforation behaviour of CFRPs using high-velocity steel sphere. Int. J. Impact Eng. 2002;27(5):497-508.

[9] Tanabe Y, Aoki M, Fuji K, Kasano H, Yasuda E. Fracture behaviour of CFRPs impacted by relatively high-velocity steel sphere. Int. J. Impact Eng. 2003;28(6): 627-642.

[10] David-West O S, Alexander NV, Nash DH, Banks WM. Energy absorption and bending stiffness in CFRP laminates: The effects of 45° plies. Thin-Walled Structures 2008;46(7):860-869.

[11] Cantwell WJ, Morton J. Comparison of the low and high velocity impact response of CFRP. Composities 1989;20(6):545-551.

[12] Hazell PJ, Kister G, Stennett C, Bourque P, Cooper G. Normal and oblique penetration of woven CFRP laminates by a high velocity steel sphere. Composites Part A 2008;39:866-874.

[13] Caprino G, Lopresto V, Santoro D. Ballistic impact behaviour of stitched graphite/epoxy laminates. Compos. Sci. and Tech. 2007;67:325-335.

[14] López-Puente J, Zaera R, Navarro C. Experimental and numerical analysis of normal and oblique ballistic impacts on thin carbon/epoxy woven laminates. Composites Part A: Applied Science and Manufacturing 2008;39(2):374-387.

[15] Reid SR, Wen HM. Perforation of FRP laminates and sandwich panels subjected to missile impact. Cambridge: Woodhead Publishing Limited, 2000.

[16] Cantwell WJ, Morton J. Impact perforation of carbon fibre reinforced plastic. Compos. Sci. Technol. 1990;38:119-141.

[17] Robinson P, Davies GAO. Impactor mass and specimen geometry effects in low velocity impact of laminated composites. Int. J. Impact Eng. 1992;12(2):189-207.

[18] Wen HM. Predicting the penetration and perforation of FRP laminates struck normally by the projectiles with different nose shapes. Compos. Struct. 2000;49:321-329.

[19] Wu QG, Wen HM, Qin Y, Xin SH. Perforation of FRP laminates under impact by flat-nosed projectiles. Composites: Part B. 2012;43:221-227.

[20] Naik NK, Shrirao P. Composite structures under ballistic impact. Composite Structures 2004;66:579-590.

[21] Naik NK, Shrirao P, Reddy BCK. Ballistic impact behavior of woven fabric composites: Parametric studies. Mater. Sci. and Eng. A 2005;412:104-116.

[22] Shaktivesh, Nair NS, Sesha Kumar ChV, Naik NK. Ballistic impact performance of composite targets. Mater. and Design 2013;51:833-846.

[23] Varas D, Artero-Guerrero JA, Pernas-Sánchez J, López-Puente J. Analysis of high velocity impacts of steel cylinders on thin carbon/epoxy woven laminates. Composite Structures 2013;95:623-629.

[24] Appleby-Thomas GJ, Hazell PJ, Stennett C. The variation in lateral and longitudinal stress gauge response within an RTM 6 epoxy resin under one-dimensional shock loading. J. Mater. Sci. 2009;44(22):6187-6198.

[25] Hazell PJ, Appleby-Thomas G. A study on the energy dissipation of several different CFRP-based targets completely penetrated by a high velocity projectile. Compos. Struct. 2009;91(1):103-109.

[26] Hazell PJ, Cowie A, Kister G, Stennett C, Cooper GA. Penetration of a woven CFRP laminate by a high velocity steel sphere impacting at velocities of up to 1875 m/s. Int. J. of Impact Engng. 2009;36:1136-1142.

[27] Hazell PJ. Ceramic Armour: Design and Defeat Mechanisms. Canberra, Australia: Argos Press, 2006.

A study of the penetration behaviour of mild-steel-cored ammunition against boron carbide ceramic armours

Crouch, Ian G.

2015-03-13

Crouch IG, Appleby-Thomas G, Hazell PJ. A study of the penetration behaviour of mild-steel-cored ammunition against boron carbide ceramic armours. International Journal of Impact Engineering Volume 80, June 2015, pp. 203-211

https://doi.org/10.1016/j.ijimpeng.2015.03.002